Looking into DNA breathing dynamics via quantum physics

Lian-Ao Wu,[1] Stephen S. Wu,[2] and Dvira Segal[3]
[1]*Ikerbasque-Basque Foundation for Science and Department of Theoretical Physics and History of Science, The Basque Country University (EHU/UPV), P.O. Box 644, 48080 Bilbao, Spain*
[2]*Department of Life Science, Queen's University, Kingston, Ontario, Canada K7L 3N6*
[3]*Department of Chemistry and Center for Quantum Information and Quantum Control, University of Toronto, 80 St. George Street, Toronto, Ontario, Canada M5S 3H6*
(Received 27 February 2009; published 1 June 2009)

We study generic aspects of bubble dynamics in DNA under time-dependent perturbations, for example, temperature change, by mapping the associated Fokker-Planck equation to a quantum *time-dependent* Schrödinger equation with imaginary time. In the static case we show that the eigenequation is exactly the same as that of the β-deformed nuclear liquid drop model, without the issue of noninteger angular momentum. A universal breathing dynamics is demonstrated by using an approximate method in quantum mechanics. The calculated bubble autocorrelation function qualitatively agrees with experimental data. Under time-dependent modulations, utilizing the adiabatic approximation, bubble properties reveal memory effects.

DOI: 10.1103/PhysRevE.79.061901 PACS number(s): 87.14.gk, 02.50.−r, 05.40.−a, 87.10.Mn

I. INTRODUCTION

The stability of the double helix structure of DNA can be attributed to the phosphodiester bonds in the single-stranded sugar backbone and hydrogen bonds between complementary base pairs of opposite strands. However, the hydrogen bonds between parallel strands can be locally broken under physiological conditions preceding events such as DNA replication, transcription, denaturation, and protein binding [1]. A change in environmental conditions such as *p*H or temperature may provide the energy required to *progressively* open the hydrogen bonds, producing domains of single-stranded DNA (bubbles). Eventually, e.g., upon heating, denaturation occurs and the two strands separate altogether. Understanding the underlying mechanisms behind breathing fluctuations [2] and force-assisted denaturation [3] may provide further insights onto DNA structure and function.

Breathing dynamics was recently detected through fluorescence fluctuations in a tagged double-stranded DNA [4]. Various treatments were employed for simulating this effect: the master-equation approach [5,6], stochastic dynamic simulations of the Dauxois-Peyrard-Bishop model [7], and by adopting the Poland-Scheraga free-energy function [8], considering the associated Fokker-Planck equation [9,10]. Specifically, it has been suggested that thermally induced breathing processes could be mapped into the quantum Coulomb problem, with noninteger orbital angular momentum [11]. Here the temperature, a parameter in the free energy, plays a role in distinguishing repulsive from attractive Coulombic potentials.

In this paper we are concerned with DNA bubble dynamics when temperature, or other control parameters, varies in time. Adopting a generic unpairing energy function, we study the bubble survival behavior based on the mapping of the Fokker-Planck equation with *time-dependent parameters* to the quantum time-dependent Schrödinger equation with imaginary time. By employing approximate quantum-mechanics methods, a universal breathing dynamics is demonstrated, insensitive to the details of the free-energy function. Moreover, we exemplify memory effects when external parameters (e.g., temperature or *p*H) are slowly varied.

II. MODEL

The Poland-Scheraga free energy for a single bubble can be written as [8,9]

$$F(x) = \Gamma(x) + ck_BT\ln(x+1) + \gamma_0, \tag{1}$$

with $x \geq 0$ as the bubble size in units of base pairs. γ_0, the free-energy barrier to form the initial bubble, is next omitted as it only introduces a constant shift in energy. The entropy loss associated with the formation of a closed polymer ring is incorporated by the factor $ck_BT\ln(x+1)$, whereas $\Gamma(x) = 2k_BT\int^x \varepsilon(y)dy$ represents the free energy for the dissociation of x base pairs [12,13], where k_B is the Boltzmann constant and T is the temperature. The function $\Gamma(x)$ or $\varepsilon(y)$ may be modeled based on experimental data. A simple model [9] assumes that $\Gamma(x) = -\gamma_1 \frac{\Delta T}{T_m} x$, where $\Delta T = T - T_m$ with T_m being the melting temperature and $\gamma_1 = 4k_BT_\gamma$; $T_\gamma = 37\ ^\circ\mathrm{C}$ is the reference temperature. Since we are interested here in the time evolution of the bubble distribution due to a change in a parameter κ, e.g., temperature or *p*H, we write $\Gamma = \Gamma(\Delta\kappa, x)$, where $\Delta\kappa = \kappa - \kappa_c$; κ_c the critical value of κ. Note that Γ should be an odd function of $\Delta\kappa$.

At a finite temperature, the one-dimensional bubble dynamics can be modeled using the overdamped Langevin equation with a Gaussian white noise [11],

$$\dot{x} = -D\frac{\partial F}{\partial x} + \eta, \quad \langle \eta(t)\eta(\tau)\rangle = 2k_BTD\delta(t-\tau), \tag{2}$$

where D is a kinetic coefficient of units $(k_BT \times \mathrm{s})^{-1}$. The corresponding probability density $P = P(x,t)$ satisfies the Fokker-Planck equation [14],

$$\frac{\partial P}{\partial t} = \frac{\partial}{\partial x}(f'P) + \frac{1}{2}\frac{\partial^2 P}{\partial x^2}, \tag{3}$$

where $f' = \partial f/\partial x$ and $f(x) = F(x)/2k_BT$. The time variable was

redefined as $2Dk_BTt \to t$. Introducing a *dressed* transformation $P=e^{-f(x)}\tilde{P}=e^{-\Gamma(x)/2k_BT}(x+1)^{-\mu}\tilde{P}$, where $\mu=c/2$, leads to

$$-\frac{\partial \tilde{P}}{\partial t}=H\tilde{P}, \quad H=-\frac{1}{2}\frac{\partial^2}{\partial x^2}+V(x,t), \tag{4}$$

with a time-dependent potential energy

$$V(x,t)=U(x)+\frac{\mu(\mu+1)}{2x^2}-\frac{\partial f}{\partial t}, \tag{5}$$

where we assumed that the time-dependent parameters are T and ε. The potential $U(x)$ is given by

$$U(x)=\frac{\varepsilon(x)^2}{2}+\frac{\mu\varepsilon(x)}{x}-\frac{\varepsilon'(x)}{2}, \tag{6}$$

assuming that $x \gg 1$. Equation (4) resembles the time-dependent Schrödinger equation with imaginary time for a particle in a time-dependent potential. For the static case the dynamics superficially resembles the radial equation of a particle in a central potential $U(x)$ with centrifugal barrier $\mu(\mu+1)/2x^2$. However, in the quantum-mechanical case the angular momentum μ must be an integer. It is thus of fundamental interest to identify a quantum system which permits real values for μ.

The Bohr Hamiltonian [15] in the nuclear liquid drop model with a mass parameter $B_2=1$ is given by ($\hbar=1$)

$$H_B=-\frac{1}{2}\left[\frac{1}{\beta^4}\frac{\partial}{\partial\beta}\beta^4\frac{\partial}{\partial\beta}-\frac{C_5(\gamma,\Omega)}{\beta^2}\right]+V(\beta,\gamma). \tag{7}$$

Here β and γ are the parameters corresponding to the shape of a nucleus as an incompressible drop with quadrupole deformation, Ω is the Euler angle onto the body-fixed axes, and $C_5(\gamma,\Omega)$ is the Casimir operator of the SO(5) group [16]. For a family of potentials $V(\beta,\gamma)=U(\beta)+V(\gamma)/\beta^2$ [17], the β degree of freedom can be separated,

$$\left[-\frac{1}{2}\frac{\partial^2}{\partial\beta^2}+U(\beta)+\frac{\mu(\mu+1)}{2\beta^2}\right]u(\beta)=Eu(\beta),$$

$$[C_5(\gamma,\Omega)+2V(\gamma)]\varphi(\gamma,\Omega)=[\mu(\mu+1)-2]\varphi(\gamma,\Omega), \tag{8}$$

so as the Bohr Hamiltonian eigenstates are given by $u(\beta)\varphi(\gamma,\Omega)/\beta^2$. In a γ-unstable situation, $V(\gamma)=0$, where $\mu=1,2,\ldots$ are integers. However, in general situations the effective Hamiltonian $H=-\frac{1}{2}\frac{\partial^2}{\partial\beta^2}+U(\beta)+\frac{\mu(\mu+1)}{2\beta^2}$ has the exact same form as that of the breathing bubble (4) in the static case, with β replaced with x and μ is any positive number. This suggests that a nuclear liquid drop model, rather than a particle in a central potential [11], better describes bubble dynamics in double-stranded polymers.

III. STATIC LIMIT

When all variables are time independent the probability density $\tilde{P}$ of Eq. (4) can be expanded in the normalized eigenstates Ψ_n solving $H\Psi_n=E_n\Psi_n$,

$$P(x,t)=e^{-f(x)}\sum_n c_n e^{-E_n t}\Psi_n(x), \tag{9}$$

where the coefficients c_n are determined by the initial condition and the completeness of Ψ_n. We specify next the boundary conditions and distinguish between scattering potentials and binding potentials. To account for bubble closure absorbing boundary conditions are taken for vanishing bubble size, $\Psi_n(0)=0$. Likewise, for considering a complete denaturation of a long strand with a maximum bubble size L, the absorbing condition $\Psi_n(L\to\infty)=0$ is implied. In order to satisfy both conditions, the family of functions $\varepsilon(x)$ should be monotonic for large x values, so that $V(x)$ is a binding potential. For instance, if $\varepsilon(x)$ is a polynomial of degree $M>0$, the generated potential $V(x)$ [see Eqs. (5) and (6)] is always a binding potential with the asymptotic behavior

$$\frac{\mu(\mu+1)}{2x^2}\overset{x\to 0}{\longrightarrow}\infty, \quad \frac{\varepsilon(x)^2}{2}\overset{x\to\infty}{\longrightarrow}\infty.$$

In contrast, if $M=0$, $\varepsilon(x)$ is a constant corresponding to the Coulomb's potential, and the total potential is now a *scattering potential*, allowing the function $\Psi_n(L\to\infty)$ to differ from zero.

A. WKB analysis

When time approaches infinity, the transition probability (9) reads

$$P(x,t)e^{E_g t}\approx c_g e^{-f(x)}\Psi_g(x), \tag{10}$$

where $\Psi_g(x)$ is the ground state of the given potential with eigenenergy E_g. In the scattering case $\Psi_g(x)$ is an oscillating function of x, while a bound ground state is usually nodeless and localized at a certain region of x. What is the effect of the factor $e^{-f(x)}$ on the dynamics? When acting on the scattering ground state, it affects the long-time behavior of the transition probability leading to closure or denaturation of DNA bubbles [11]. On the other hand, a bound ground state $\Psi_g(x)$ approaches zero when $x\to\infty$; thus, the role of the $e^{-f(x)}$ factor becomes influential. If the speed of its divergence is slower than the convergence of $\Psi_g(x)$, the bubble tends to close rather than to denaturate, and vice versa. Qualitative analysis can be made in terms of the traditional WKB approximation [18]. The exponential factor of the ground state is given by $\Psi_g(x)\propto\exp\{-\int^x dy\sqrt{2[V(y)-E_g]}\}$; $E_g<V(y)$. In the asymptotic large x limit, the probability in (10), omitting the time-dependent part, reduces to $P(x)\propto\exp\{-\int^x dy[\varepsilon(y)+\sqrt{\varepsilon(y)^2-2E_g}]\}$. For the Coulomb potential, $\varepsilon(y)=\varepsilon_0$ is a constant; therefore, $P\propto e^{-[\varepsilon_0+|\varepsilon_0|\mu/(\mu+1)]x}$ [19]. More generally, for bound potentials, $V(x\to\infty)=\varepsilon(x)^2/2$; therefore, $\Psi_g(x\to\infty)\propto\exp[-\int^x|\varepsilon(y)|dy]$ yielding the probability distribution

$$P(x)\propto\exp\left\{-\int^x[\varepsilon(y)+|\varepsilon(y)|]dy\right\}. \tag{11}$$

Since the integrand is non-negative, $\int^x[\varepsilon(y)+|\varepsilon(y)|]dy$ either increases for $\varepsilon(y)>0$, leading to bubble closure, or does not change with x for $\varepsilon(y)<0$, so as the integrated probability

linearly scales with size. The WKB analysis thus provides a universal long-time behavior, insensitive to the details of the unpairing energy function. However, the WKB method is usually not suitable for obtaining the exact functional behavior; an example is provided below.

B. Exactly solvable example

The transition probability P from an initial bubble of size x_0 to a bubble of final size x at time t is given by Eq. (9) as

$$P(x,x_0,t) = e^{-f(x)+f(x_0)} \sum_n e^{-E_n t} \Psi_n(x) \Psi_n(x_0), \tag{12}$$

with the initial condition $P(x,x_0,0)=\delta(x-x_0)$. At long times it is approximately given by

$$P(x,x_0,t) \overset{t\to\infty}{\longrightarrow} e^{-f(x)+f(x_0)} e^{-E_g t} \Psi_g(x) \Psi_g(x_0). \tag{13}$$

In order to simplify our analysis, we consider the following expansion for the unpairing function: $\varepsilon(x)=\varepsilon_0+2\varepsilon_1 x+O(x^2)$. Truncating the series after the linear term results in $\Gamma(x)=2k_BT(\varepsilon_0 x+\varepsilon_1 x^2)$, generating the potential $U(x)=2\varepsilon_1^2 x^2+2\varepsilon_1\varepsilon_0 x+\frac{\mu\varepsilon_0}{x}+\frac{\varepsilon_0^2+2\varepsilon_1(2\mu-1)}{2}$ [see Eq. (6)]. If $\varepsilon_1=0$, the potential reduces to the Coulomb potential as in [11]. However, since the effect of ε_1 dominates at large distances, one should consider its contribution, for example, by using a perturbation series [20]. For simplicity we assume next that $\varepsilon_0=0$, resulting in the spiked harmonic-oscillator potential (5)

$$V(x) = 2\varepsilon_1^2 x^2 + \varepsilon_1(2\mu-1) + \frac{\mu(\mu+1)}{2x^2}, \tag{14}$$

with the exact ground state [21]

$$\Psi_g(x) = \left[\frac{\sqrt{8|\varepsilon_1|}}{\tilde{\Gamma}\left(\mu+\frac{3}{2}\right)}\right]^{1/2} (\sqrt{2|\varepsilon_1|}x)^{\mu+1} e^{-|\varepsilon_1|x^2}, \tag{15}$$

where $E_g=(3+2\mu)|\varepsilon_1|+\varepsilon_1(2\mu-1)$ and $\tilde{\Gamma}(z)$ is the gamma function. We substitute Eq. (15) into Eq. (13) and obtain

$$P(x,x_0,t\to\infty) \approx x \frac{2(2|\varepsilon_1|)^{\mu+3/2}(x_0)^{2\mu+1}}{\tilde{\Gamma}\left(\mu+\frac{3}{2}\right)} \frac{e^{-(\varepsilon_1+|\varepsilon_1|)x^2}}{e^{-(\varepsilon_1-|\varepsilon_1|)x_0^2}} e^{-E_g t}. \tag{16}$$

When $\varepsilon_1>0$, the distribution is localized near $x=0$, implying bubble closure. In contrast, for $\varepsilon_1<0$ the distribution leans toward larger x values ($P\propto x$). The WKB approximation (11) thus produced the correct exponential factor but it could not provide the factor x. The correlation function $C(t)$, proportional to the integrated survival probability, $C(t)\propto\int_0^L P(x,x_0,t)dx$, where L is the length of the DNA chain, can be recorded experimentally [4]. We explore next this quantity as well as the first passage time distribution $W(t)=-dC(t)/dt$.

We first study the $\epsilon_1>0$ case. Using sum (12) we obtain a superposition of exponentially decaying functions, corresponding to various relaxation modes [4],

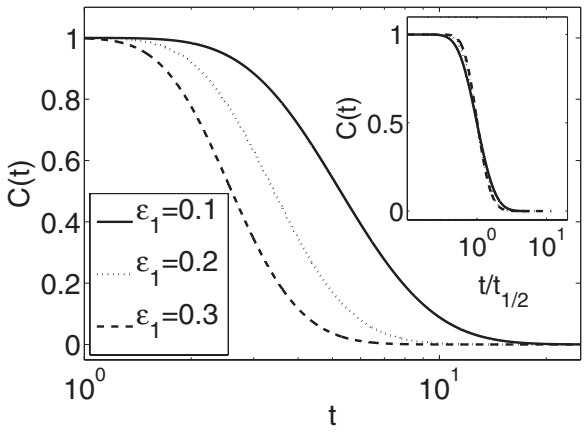

FIG. 1. Autocorrelation function at $\mu=1/2$ and $x_0=5$ [Eq. (19)] for $\varepsilon_1=0.1$ (full curve), $\varepsilon_1=0.2$ (dotted curve), and $\varepsilon_1=0.3$ (dashed curve). Inset: the curves with rescaled times $t\to t/t_{1/2}$.

$$C(t) = \frac{(2\varepsilon_1)^{\mu+1/2}x_0^{2\mu+1}}{\tilde{\Gamma}\left(\mu+\frac{3}{2}\right)\left(\mu+\frac{1}{2}\right)^{-1}} \sum_{n=0}^{\infty} \frac{\xi^{n+\mu+1/2} L_n^{\mu+1/2}(2\varepsilon_1 x_0^2)}{n+\mu+\frac{1}{2}}. \tag{17}$$

Here $\xi\equiv e^{-4\varepsilon_1 t}$ and $L_n^{\mu+1/2}$ is the associated Laguerre polynomial. The first passage time distribution could be exactly calculated, taking the time derivative of this expression. At $\mu=1/2$ it has the following form:

$$W_{\mu=1/2}(t) = 8(\varepsilon_1 x_0)^2 \frac{e^{-4\varepsilon_1 t} \exp\left[\frac{2\varepsilon_1 x_0^2}{1-\exp(4\varepsilon_1 t)}\right]}{[1-\exp(-4\varepsilon_1 t)]^2}, \tag{18}$$

with $W(0)=W(\infty)=0$, and a maximum in between, resulting in a profile similar to that obtained in [11]. The correlation function at $\mu=1/2$ is given by

$$C_{\mu=1/2}(t) \propto 1-\exp\left[\frac{2\varepsilon_1 x_0^2}{1-\exp(4\varepsilon_1 t)}\right], \tag{19}$$

with the long-time limit $C_{\mu=1/2}(t)\propto e^{-4\varepsilon_1 t}$. The bubble lifetime is therefore given by $\tau_c=1/4\varepsilon_1$ or $\tau_c=[4\varepsilon_1(\mu+\frac{1}{2})]^{-1}$ in general cases [see Eq. (17)]. On the other hand, at short times, $C_{\mu=1/2}(t)\propto 1-\exp(-x_0^2/2t)$. Figure 1 presents the correlation function using the analytical form $\varepsilon(x)=2\varepsilon_1 x$ for the unpairing free energy and $\mu=1/2$ [see Eq. (1)]. Notice that the curves at different ε_1, corresponding, e.g., to different temperatures or DNA structures, follow the same universal temporal behavior. When presented as a function of a rescaled time [$t\to t/t_{1/2}$, where $C(t_{1/2})=\frac{1}{2}$], the plots collapse into a single curve, in a good agreement with experiments [4] and other theoretical treatments [6,22]. Incorporating ε_0 should result in a similar behavior.

We show next results for $\epsilon_1<0$. In this case the DNA fully denatures at long times and correlations diverge. At $\mu=1/2$ we can exactly obtain the first passage time distribution

$$W_{\mu=1/2}(t) = \frac{8(\varepsilon_1 x_0)^2}{e^{4|\varepsilon_1|t} - 1}\left\{1 - \exp\left[-\frac{2|\varepsilon_1|L^2}{\exp(4|\varepsilon_1|t) - 1}\right]\right\} \tag{20}$$

and the corresponding correlation function $C(t)$. At long times both scale as L^2.

IV. TIME-DEPENDENT EFFECTS

The adiabatic approximation is standardly applied to describe the dynamic of systems under slowly varying time-dependent Hamiltonians [18]. Since the relaxation time of the bubble, on the order of μs [4], is typically shorter than the modulation time of a parameter κ, e.g., the temperature, the quantum adiabatic approximation may be applied to describe the dynamics in the imaginary-time Schrödinger equation (4). Defining an instantaneous basis of eigenenergies $H(t)|n(t)\rangle = E_n(t)|n(t)\rangle$, we obtain $\langle n|\dot{k}\rangle = \frac{\langle n|\dot{H}|k\rangle}{\omega_{kn}}$, where $\omega_{kn}(t) = E_k(t) - E_n(t)$. In the axial representation the wave function is written as $|\Psi(t)\rangle = \Sigma_n a_n(t)\exp[-\int_0^t d\tau\, E_n(\tau)]|n(t)\rangle$. Substituting this into the imaginary-time Schrödinger, equation we get

$$\dot{a}_n = -a_n\langle n|\dot{n}\rangle - \sum_{k\neq n} a_k(t)\frac{\langle n|\dot{H}|k\rangle}{\omega_{kn}}\exp\left[-\int_0^t d\tau\, \omega_{kn}(\tau)\right]. \tag{21}$$

Under the adiabatic approximation, the coefficients $a_n(t)$ evolve independently from each other since couplings between states are negligible [18]. In the present case we require that $\left|\frac{\langle n|\dot{H}|k\rangle}{\omega_{kn}}\right|\exp[-\int_0^t d\tau\, \omega_{kn}(\tau)] \ll 1$. If $\omega_{kn}(t) > 0$, the exponential factor is always less than 1, while for $\omega_{kn} < 0$ it may diverge at long times. Therefore, the applicability of the adiabatic approximation may be questionable for general instantaneous states [23], yet for the ground state it is valid as long as the standard adiabatic condition $\left|\frac{\langle n|\dot{H}|k\rangle}{\omega_{kn}}\right| \ll 1$ holds. Under the adiabatic approximation the ground-state amplitude evolves according to $\dot{a}_g \approx -a_g\langle g|\dot{g}\rangle$. However, since $\langle n|\dot{n}\rangle$ is zero for any one-dimensional real wave function, the overall function propagates as $\Psi(x,t) \sim \Psi_g(x,t)\exp[-\int_0^t d\tau\, E_g(\tau)]$ with $\Psi_g(x,t)$ as the instantaneous solution. Consider, for example, the potential $V(x,t) = (2\varepsilon_1^2 - \dot{\varepsilon}_1)x^2 + \varepsilon_1(2\mu - 1) + \frac{\mu(\mu+1)}{2x^2}$ [see Eqs. (4)–(6) and (14)], which has analytical instantaneous eigenstates. To simplify, we further assume that the system initially occupies the ground state of the potential $V(x,t=0)$. Under the adiabatic approximation,

$$P(x,t) \approx \frac{(2\sigma - 2\varepsilon_1)^{\mu/2+3/4}}{\sqrt{\tilde{\Gamma}\left(\mu + \frac{3}{2}\right)/2}} x e^{-\sigma x^2}\exp\left[-\int_0^t d\tau\, E_g(\tau)\right], \tag{22}$$

with the width parameter $\sigma = \varepsilon_1 + (\varepsilon_1^2 - \frac{\dot{\varepsilon}_1}{2})^{1/2}$ and $E_g(\tau) = \sigma(\tau)(2\mu+3) - 4\varepsilon_1(\tau)$. Rich information can be obtained due to the time-dependent evolution of ε_1. First, both the width of the distribution and the peak position depend on $\dot{\varepsilon}_1$, the rate at which the external parameters (e.g., temperature) is changed. Second, the processes of increasing and decreasing the control parameter may reach the same value ε_1, yet they may result in different shapes of the bubble distribution. Specifically, the correlation function $C(t) \propto (\sigma - \varepsilon_1)^{\mu/2+3/4} \times (1 - e^{-\sigma L^2})\exp[-\int_0^t d\tau\, E_g(\tau)]$ includes the decay factor $\exp[-\int_0^t d\tau\, E_g(\tau)]$ which memorizes the different pathways that $\varepsilon_1(t)$ undergoes. For example, the two paths $\varepsilon_1(t) = 1 + t/100$ and $\varepsilon_1(t) = 1 + t^2/100$ attain the same value at $t=1$, yet the values of $\int_0^t d\tau\, E_g(\tau)$ are obviously different, yielding distinct characteristic decay times. We expect that this theoretical result could be observed experimentally.

V. SUMMARY

The dynamics of a single DNA bubble under time-dependent perturbations was studied by mapping the associated Fokker-Planck equation to a quantum time-dependent Schrödinger equation with imaginary time. For a generic unbinding free-energy function, we analyzed bubble breathing by using the WKB approximation, observing a universal behavior. Specifically, a spiked harmonic-oscillator potential yielded results in qualitative agreement with experimental data. Under slow time-dependent modulations of, e.g., the temperature or *p*H, bubble dynamics reflects memory effects.

ACKNOWLEDGMENTS

L.A.W. was supported by the Ikerbasque Foundation. D.S. acknowledges the University of Toronto start-up grant.

[1] M. D. Frank-Kamenetskii, Phys. Rep. **288**, 13 (1997).
[2] D. Poland and H. A. Scheraga, *Theory of Helix-Coil Transitions in Bio-Polymers* (Academic, New York, 1970).
[3] C. Danilowicz, Y. Kafri, R. S. Conroy, V. W. Coljee, J. Weeks, and M. Prentiss, Phys. Rev. Lett. **93**, 078101 (2004).
[4] G. Altan-Bonnet, A. Libchaber, and O. Krichevsky, Phys. Rev. Lett. **90**, 138101 (2003).
[5] H. Kunz, R. Livi, and A. Süto, J. Stat. Mech.: Theory Exp. **2007**, P06004 (2007).
[6] T. Ambjörnsson, S. K. Banik, M. A. Lomholt, and R. Metzler, Phys. Rev. E **75**, 021908 (2007).
[7] T. Dauxois, M. Peyrard, and A. R. Bishop, Phys. Rev. E **47**, R44 (1993).
[8] D. Poland and H. A. Scheraga, J. Chem. Phys. **45**, 1456 (1966).
[9] A. Hanke and R. Metzler, J. Phys. A **36**, L473 (2003).
[10] A. Bar, Y. Kafri, and D. Mukamel, Phys. Rev. Lett. **98**, 038103 (2007).
[11] H. C. Fogedby and R. Metzler, Phys. Rev. Lett. **98**, 070601 (2007); Phys. Rev. E **76**, 061915 (2007).

[12] Zh. S. Gevorkian and C.-K. Hu, e-print arXiv:0810.0755.
[13] For convenience, temperature appears as a prefactor in Γ. In comparison to [12], our $\varepsilon(x)$ compensates this factor.
[14] S. I. Denisov, W. Horsthemke, and P. Hänggi, Eur. Phys. J. B **68**, 567 (2009).
[15] A. Bohr and B. Mottelson, *Nuclear Structure* (Benjamin, New York, 1975), Vol. 2, pp. 24–26.
[16] L. Wilets and M. Jean, Phys. Rev. **102**, 788 (1956).
[17] L. A. Wu, H. M. Ding, Z. T. Yan, and G. Liu, Phys. Rev. Lett. **76**, 4132 (1996).
[18] D. Bohm, *Quantum Theory* (Dover, New York, 1989).
[19] Our sign notation with respect to attractive and repulsive potentials is opposite to [11].
[20] N. Saad and R. L. Hall, J. Phys. A **35**, 4105 (2002).
[21] R. L. Hall, N. Saad, and A. B. von Keviczky, J. Math. Phys. **43**, 94 (2002).
[22] D. J. Bicout and E. Kats, Phys. Rev. E **70**, 010902(R) (2004).
[23] M. S. Sarandy and D. A. Lidar, Phys. Rev. A **71**, 012331 (2005).